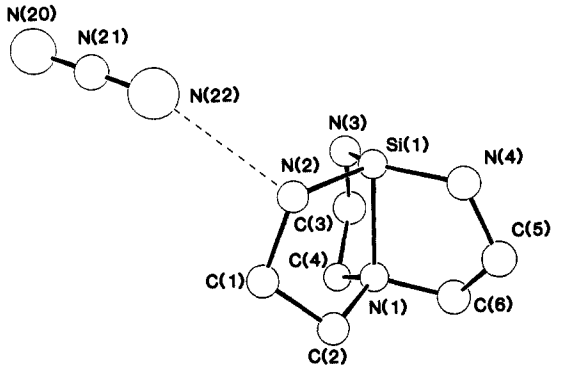

Figure 1. ORTEP drawing of one of the cations (**6**) and azide anions in **8**. Electron probability spheres are drawn at the 50% level.

in 49% yield.[5] Products **9–11**[6,7] arise presumably by nucleophilic attack of **7** on Me_3SiN_3, thereby releasing HN_3, which then reacts

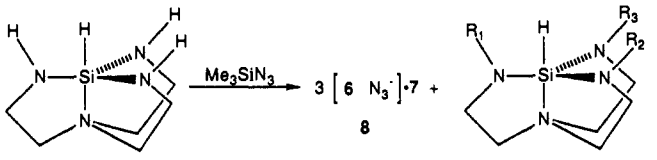

9 $R^1 = R^2 = H$, $R^3 = SiMe_3$
10 $R^1 = H$, $R^2 = R^3 = SiMe$
11 $R^1 = R^2 = R^3 = SiMe_3$

with unreacted **7** to yield **8**. X-ray diffraction studies[8] on **8** reveal the presence of cations **6** (Figure 1) and azide ions. From Figure 1 it is seen that one nitrogen of the azide ion lies within hydrogen bonding distance (283 pm, average) of the protonated nitrogen in cation **6**. Whereas the azido groups in covalent silyl and organic azides are usually bent,[9] those in **8** are essentially linear, with an average NNN angle of 178.2°. The average bond lengths (114 and 118 pm) in the azide ions of **8** are close to those reported for covalent silyl azides but also for the free azide ion.[9] Although the hydrogen atoms in **8** could not be located, the site of protonation is signalled by a significantly longer SiN(2) bond (189 pm, average) compared with the two other $Si-N_{eq}$ bond lengths (169 pm, average) in cation **6** and the $Si-N_{eq}$ bond lengths (173 pm, average) in the cocrystallized molecule of **7**. The $Si-N_{ax}$ bond lengths (208 pm) in the protonated and in the neutral silatrane molecule of **8** are equal. The constitution of **8** is further confirmed by its IR, chemical ionization mass, ^1H NMR, and solid-state ^{29}Si NMR spectra.[5] The latter spectrum exhibits resonances at -83.0 and -86.3 ppm (ratio 1:3) characteristic of pentacoordinated silicon in the neutral and protonated azasilatrane molecule, respectively, the chemical shift value of the former being in excellent agreement with that reported for **7** in solution (-82.3 ppm).[10]

Attempts to generate cation **6** by protonation of **7** with CF_3SO_3H or, indirectly, by reacting **7** with the strong electrophiles CF_3SO_3Me or $CF_3SO_3SiMe_3$ resulted in the destruction of the atrane moiety of **7**.

Acknowledgment. We thank the AFOSR for financial support and the W. R. Grace company for samples of tren.

Supplementary Material Available: Description of the data collection and structure solution and tables of positional and isotropic thermal parameters, bond distances and angles, and least-squares planes (14 pages); a listing of observed and calculated structure factors (10 pages). Ordering information is given on any current masthead page.

(5) To a filtered solution of 0.71 g (4.1 mmol) of **7** in 20 mL of dry CH_3CN was added 0.55 mL (4.2 mmol) of Me_3SiN_3. Over a period of ca. 2 h, crystalline **8** was formed (mp 138–140 °C dec; FT-IR (KBr, cm^{-1}) 3375 m, 3325 m, 2900 s (br, NH str), 2000 s (br, N≡N and SiH str); MS (Cl, NH_3) 214 (1.1%, M + 1 of $N_3Si(HNCH_2CH_2)_3N$), 173 (100%, M^+ of **6** or M + 1 of **7**); MS (Cl, CH_4) 341 (2%, M + 1 of $C_{12}H_{26}N_8Si_2$), 213 (0.5% M^+ of $N_3Si(HNCH_2CH_2)_3N$), 173 (59%, M^+ of **6** or M + 1 of **7**), 171 (100%, M^+ - 2 of **6** or M^+ - 1 of **7**); ^1H NMR ($CDCl_3$): 2.61 t, 2.86 t (CH_2 cage protons of **7**), 2.65 t, 2.99 t (CH_2 cage protons of **6**, ratio cage proton sets of **7**:**6** = 1:3), 4.27 s (br, NH, NH_2), 4.67 s (SiH of **6**). Elemental anal. Calcd (found) for $C_{24}H_{67}N_{25}Si_4$: C, 35.44 (35.22); H, 8.25 (8.56); N, 42.79 (42.79); Si, 13.73 (13.45).

(6) Compounds in the supernatant were characterized by GLC, high-resolution mass spectroscopy, and ^1H NMR (yield (GC-MS): **8**, 17%; **10**, 47%; **11**, 26%; **12**, 10%). Authentic samples of **10** and **11** were available for comparison (see ref 7).

(7) (a) Gudat, D.; Daniels, L. M.; Verkade, J. G. *J. Am. Chem. Soc.* **1989**, *111*, 8520. (b) Gudat, D.; Verkade, J. G. *Organometallics* **1989**, *8*, 2772.

(8) **7**: monoclinic, space group *Ia*, $Z = 4$; $a = 13.400$ (3) Å, $b = 22.645$ (3) Å, $c = 13.812$ (2) Å; $\beta = 108.85$ (1)°; $V = 3966$ (1) Å^3; $d_{calcd} = 1.370$ g/cm^3; $4° < 2\theta < 45°$, (Mo Kα, λ) = 0.71073 Å; $\mu = 1.99$ cm^{-1}). A total of 2588 unique reflections collected at -20 °C were used to solve (direct methods) the structure; 1823 reflections having $I > 3\sigma(I)$ were used in the refinement, which converged to $R = 5.98\%$, $R_w = 7.48\%$ ($w = 1/(\sigma^2(|F_o|))$). Non-hydrogen atoms were refined with isotropic temperature factors. Hydrogen atoms were used in idealized positions for the carbon atoms only. Details are given in the supplementary material.

(9) Zigler, S. S.; Haller, K. J.; West, R. *Organometallics* **1989**, *8*, 1656 and references cited therein.

(10) Kupce, E.; Liepins, E.; Lapsina, G.; Zelcans, G.; Lukevics, E. *J. Organomet. Chem.* **1987**, *333*, 1.

Ketone Perfluoroenolates: Regioselective and Stereoselective Synthesis, Unique Reactivities, and Electronic Properties

Cheng-Ping Qian and Takeshi Nakai*

Department of Chemical Technology
Tokyo Institute of Technology, Meguro, Tokyo 152, Japan

David A. Dixon and Bruce E. Smart*

Contribution No. 5366
Central Research & Development Department
E. I. du Pont de Nemours & Co.
Wilmington, Delaware 19880-0328

Received December 11, 1989

Despite the prominent role of metal enolates in organic synthesis, the chemistry of perfluoroenolates (*F*-enolates) remains relatively unexplored. We recently introduced a new, practical method to generate the parent ketone *F*-enolate **1** and described its unique spectrum of reactivity.[1] For this method to be generally useful in organofluorine synthesis, its scope and other fundamental aspects of *F*-enolate chemistry need to be explored. We now report the highly regio- and stereoselective generation of β-trifluoromethyl-substituted *F*-enolates **2**, whose kinetic reactivities differ significantly from those of **1**.

The regio- and stereoselectivities observed in the generation of **2** from alcohols **3**[2] (eq 1) are summarized in Table I. For the Li enolates (entries 1–5), only the *Z* isomers are formed in ether, whereas in THF the selectivity decreases and in THF/HMPA it reverses to favor the *E* isomer. "Internal" enolates **2b** are produced almost exclusively, irrespective of solvent and metal ion

(1) Qian, C.-P.; Nakai, T. *Tetrahedron Lett.* **1988**, *29*, 4119.

(2) The alcohols **3** were obtained in ca. 70% distilled yields by $LiAlH_4$ reduction of the corresponding *F*-ketones, which were prepared from R_fCO_2Et and CF_3CF_2I according to the literature procedure: Chen, L. S.; Chen, G. J.; Tamborski, C. *J. Fluorine Chem.* **1984**, *26*, 341.

0002-7863/90/1512-4602$02.50/0

Table I. Regioselectivity and Stereoselectivity of *F*-Enolate Formation

entry	alcohol	M[a]	solvent	isomeric ratio[b] (*Z*)-**2**:(*E*)-**2**:**4**	yield,[b] %
1	**3a**	Li	Et_2O	100:0	81
2		Li	THF	79:21	74
3	**3b**	Li	Et_2O	88:0:12	82
4		Li	THF	87:13:0	68
5		Li	THF/HMPA[c]	40:60:0[d]	68
6		K	Et_2O	100:0:0	78
7		K	THF	65:35:0	71

[a] Run at −70 °C for 4 h using 2.2 equiv of *n*-BuLi for **2** (M = Li) or 1.2 equiv of KH followed by 1.1 equiv of *n*-BuLi for **2** (M = K). [b] Determined by ^{19}F NMR after trapping with AcCl for **2a** or with MEMCl for **2b**. The isomeric *F*-enol acetates and ethers are clearly distinguishable by ^{19}F NMR, particularly by the multiplicity of the β-CF_3 signals (see the supplementary material). [c] THF:HMPA = 4:1 by volume. [d] (*Z*)-**2b**:(*E*)-**2b**:**4** = 38:58:4 from Me_3SiCl trapping experiments.

Scheme I

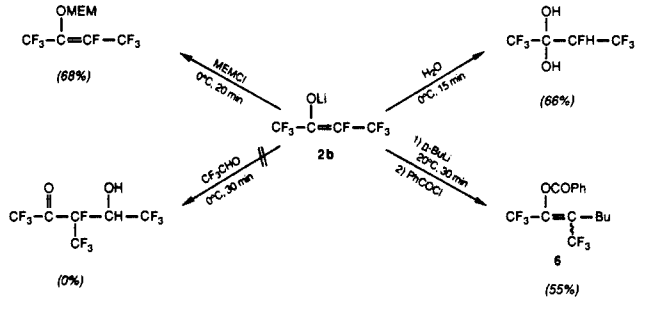

employed, except for the reaction with *n*-BuLi in ether, which gives appreciable "terminal" enolate **4** (entry 3).[3] Notably, (*Z*)-**2b** (M = K) is formed both regio- and stereospecifically in ether.

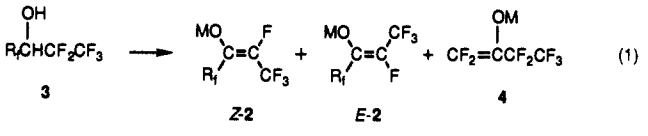

(**a**, $R_f = CF_2CF_3$; **b**, $R_f = CF_3$)

The increase in *Z* stereoselectivity with decreasing solvent coordination to Li (HMPA > THF > ether)[4a] indicates that stereoselectivity is controlled by the extent of internal F → Li coordination in the Li alkoxide intermediate.[4b] Trans HF elimination thus would likely proceed exclusively through species A in ether, but partially through B in THF and more so in THF/HMPA.[5] Alternatively, syn elimination must involve C (vs D) to account for the *Z* stereospecificity. Although at this time we cannot distinguish between trans vs syn elimination pathways, either counterintuitively requires elimination of F that is *not* coordinated to Li.[6,7]

Table II. Electronic Properties of Free *F*-Enolates[a]

enolate	charge (e) on α-C	β-C	O	HOMO (eV)	LUMO (eV)
$CH_3C_\alpha(O^-)=C_\beta H_2$ (**5**)	0.44	−0.82	−0.63	−1.83	11.60
$CF_3C_\alpha(O^-)=C_\beta F_2$ (**1**)	0.11	0.18	−0.61	−3.45	10.03
(*Z*)-$CF_3C_\alpha(O^-)=C_\beta FCF_3$ (**2b**)	0.21	−0.09	−0.53	−4.43	8.61
(*E*)-**2b**	0.19	−0.13	−0.53	−4.45	8.52

[a] Calculated at the optimized geometry obtained with a doublet-ζ basis set augmented by *d* functions on C and O.[9,10] See supplementary material for the molecular coordinates.

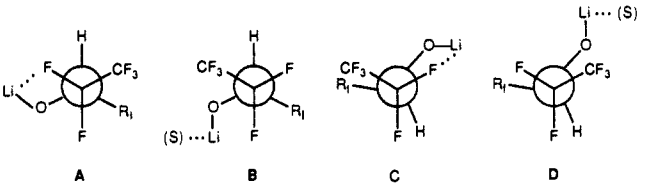

The reactions of **2b** (M = Li) in ether with various electrophiles and nucleophiles are shown in Scheme I. With (2-methoxyethoxy)methyl chloride (MEMCl) and H_2O, **2b** affords the same type of products as **1**, albeit in slightly lower yields. In contrast to the high aldol reactivity of **1**, however, **2b** does not react with aldehydes, even CF_3CHO.[8] Moreover, the unusual C-electrophilicity of **2b** is distinctly greater than that of **1**, judging by the much higher yield for its reaction with *n*-BuLi to afford, after benzoylation, the β-butyl *F*-enol benzoate **6**.[9] These significant differences in reactivity are well accommodated by frontier molecular oribtal theory.

The calculated electronic properties of the *F*-enolates and the hydrocarbon reference **5** are compared in Table II.[10,11] The most revealing features are as follows: (a) the oxygen charge densities of the *F*-enolates and **5** are very similar, (b) the β-carbons of the *F*-enolates no longer have a large negative charge, and (c) the HOMO[12] and LUMO are both significantly stabilized in **1** vs **5**

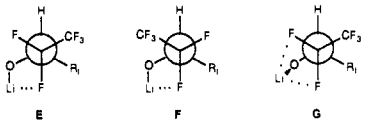

(3) "Internal" enolate formation is expected to be favored both kinetically and thermodynamically. Under identical reaction conditions [*n*-BuLi (2.1 equiv), THF, −78 °C, 4 h], 100% *F*-enolate is formed from $(CF_3CF_2)_2CHOH$ but only 37% from $(CF_3)_2CHOH$. The relative stability of the free enolates (gas phase) is (*E*)-$CF_3C(O^-)=CFCF_3$ (0) > (*Z*)-$CF_3C(O^-)=CFCF_3$ (5.6) > $CF_2=C(O^-)CF_2CF_3$ (26.3 kcal/mol) from ab initio calculations. Control experiments, however, rule out any equilibrations under our reaction conditions, and therefore the observed isomer ratios in Table I are the kinetic product distributions.

(4) (a) See: Reichardt, C. *Solvents and Solvent Effects in Organic Chemistry*; VCH Publishers: New York, 1988; Chapters 2 and 5 and references therein. (b) For a pertinent discussion on the importance of alkali metal coordination of fluorine, see ref 1 and see: Carrell, H. L.; Clusker, J. P.; Pierce, E. A.; Stallings, W. D.; Zacharias, D. E.; David, R. C.; Ashbury, C.; Konnard, C. H. L. *J. Am. Chem. Soc.* **1987**, *109*, 8067. The internal F → Li coordination is expected to compete most favorably with solvent coordination in the case of the weakest solvent ligand for lithium, diethyl ether.[4a]

(5) *F*-Enol ether produced from $CF_3CH(OMEM)CF_2CF_3$ with LDA in THF, where internal Li → F coordination cannot be operative, shows a similar *Z*:*E* ratio of 1:3 (cf. entry 5, Table I).

(6) Coordination of F to Li should assist its departure, and trans elimination ordinarily would be expected to involve E rather than A. Elimination via F, however, then should be even more favorable, but this incorrectly gives (*E*)-enolate. We therefore conclude that a trans elimination process must involve A to account for the experimental results. A reviewer, however, has proposed an interesting alternative possibility of internal lithium coordination by both gauche fluorines (G). We plan to carry out ab initio calculations on the model structures HCF_2CH_2OLi and $CF_3CF_2CH_2OLi$ to assess the importance of mono- vs bidentate F coordination.

(7) This analysis for monomeric species is obviously oversimplified since these species likely exist as aggregates, especially in diethyl ether. See, for example: Seebach, D. *Angew. Chem., Int. Ed. Engl.* **1988**, *100*, 1685.

(8) Under identical conditions (Scheme I), **1** reacts with CF_3CHO to give the aldol hydrate in 87% yield.

(9) *F*-Enolate **1** affords only a 28% yield of $CF_3C(OCOPh)=CFBu$ under the same reaction conditions.

(10) All calculations were carried out with the program GRADSCF, which is an ab initio program system designed and written by A. Kormornicki at Polyatomics Research, Mountain View, CA. The present calculations apply to free enolates in the gas phase. Similar calculations on the Li enolates to clarify the role of F → Li coordination are in progress.

(11) The basis set is from Dunning and Hay (Dunning, T. H.; Hay, P. J. In *Methods of Electronic Structure Theory*; Schaefer, H. F., III, Ed.; Plenum Press: New York, 1977; Chapter 1) and has the form (9,5,1/9,5/4)/[3,2,1/3,2/2] in the order C,O/F/H. This basis set well describes energetics, structures, and charge distributions for a variety of fluorinated anions: (a) Farnham, W. B.; Dixon, D. A.; Calabrese, J. C. *J. Am. Chem. Soc.* **1988**, *110*, 8453. (b) Farnham, W. B.; Dixon, D. A.; Calabrese, J. C. *J. Am. Chem. Soc.* **1988**, *110*, 2607. (c) Dixon, D. A.; Fukunaga, T.; Smart, B. E. *J. Am. Chem. Soc.* **1986**, *108*, 4027. (d) Farnham, W. B.; Smart, B. E.; Middleton, W. J.; Calabrese, J. C.; Dixon, D. A. *J. Am. Chem. Soc.* **1985**, *107*, 4565.

and in **2b** vs **1**. The β-C electrophilicity of the *F*-enolates is rationalized by their relatively low lying LUMOs combined with the small positive or slightly negative charge on their β-carbon atoms. The lower LUMO level of **2b** relative to that of **1** nicely accounts for its enhanced C-electrophilicity, and its comparatively *lower* HOMO level is consistent with its aldol unreactivity.[7]

In conclusion, the procedure described herein provides a facile synthesis of *F*-enolates whose reactivities markedly differ from those of their hydrocarbon analogues but can be anticipated by ab initio molecular orbital calculations. Further studies on the mechanism of enolate formation and synthetic utility are in progress.

Acknowledgment. This research was partially supported by a Grant-in-Aid for Scientific Research from the Ministry of Education, Japan, and the Chemical Materials Research & Development Foundation, which are gratefully acknowledged. We also thank Asahi Glass Company for the gift of C_2F_5I.

Supplementary Material Available: Experimental details for generating the *F*-enolates and their reactions, spectral characterization of the products, and the computed atom coordinates for the enolates (4 pages). Ordering information is given on any current masthead page.

(12) The HOMOs of these enolates have the largest electron densities in the out-of-plane p orbitals on O and C_β. There is some delocalization into the out-of-plane p orbitals bonded to C_β.

Nickel-Mediated Sequence-Specific Oxidative Cleavage of DNA by a Designed Metalloprotein

David P. Mack and Peter B. Dervan*

Arnold and Mabel Beckman Laboratories of Chemical Synthesis
California Institute of Technology
Pasadena, California 91125

Received February 13, 1990

We recently designed a sequence-specific DNA-cleaving metalloprotein consisting wholly of naturally occurring α-amino acids.[1] *The tripeptide copper-binding domain, Gly-Gly-His* (GGH), was attached to the NH_2-terminus of the DNA-binding domain of Hin recombinase (residues 139–190) to afford a new 55-residue protein, GGH(Hin139–190).[1] This protein is capable of binding DNA at four 13 base pair sites (termed *hixL* and secondary).[1] Cu·GGH(Hin139–190) in the presence of excess hydrogen peroxide and sodium ascorbate cleaves DNA predominantly at one of the four Hin binding sites.[1] We report here that, in the presence of $Ni(OAc)_2$ and monoperoxyphthalic acid, the sequence specificity and efficiency of the DNA cleavage by GGH(Hin139–190) are remarkably altered. The nickel-mediated DNA cleavage process occurs at all four binding sites, is more rapid and efficient, and is chemically activated by 1 equiv of an oxygen atom donor. At the *hixL* site, cleavage occurs predominantly at a *single* deoxyribose position on *one strand* of each binding site, indicating a nondiffusible oxidizing species.

From X-ray diffraction analysis, the tripeptide GGH is known to bind Cu(II) in a square-planar complex with coordination from an imidazole nitrogen, two deprotonated peptide nitrogens, and the terminal amino group (Figure 1).[2] Although a crystal structure of GGH·Ni(II) is not available, the Ni(II) complex of GGH has been studied by other techniques.[3-5] Crystal structures of tetraglycine with Cu(II) or Ni(II) indicate that the metal ions are bound by peptide ligands in a similar fashion.[6-8]

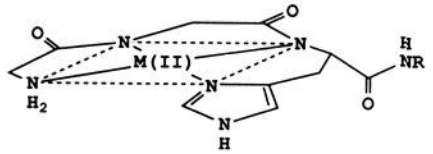

Figure 1. Model for GGH ligand bound to Cu(II) or Ni(II) in a square-planar complex[2-5] (M = Cu(II) or Ni(II)).

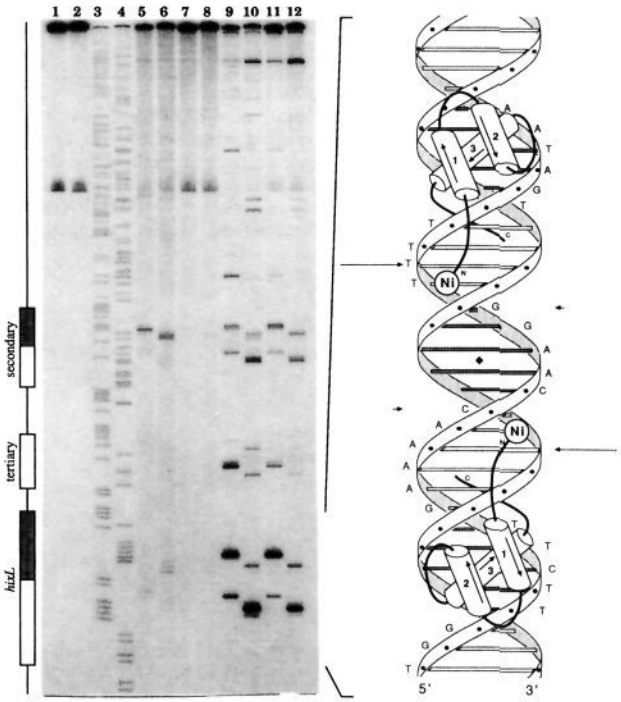

Figure 2. Left: Autoradiogram of high-resolution denaturing gel of Cu·GGH(Hin139–190) and Ni·GGH(Hin139–190) cleavage of a ^{32}P end-labeled fragment (*Xba*I/*Eco*RI) from pMFB36.[21] Reaction conditions were 20 mM NaCl, 20 mM phosphate, pH 7.5, calf thymus DNA (100 μM in base pair), and ~15 000 cpm end-labeled DNA in a total volume of 20 μL. Reactions for Cu·GGH(Hin139–190) and Ni·GGH(Hin139–190) were run for 90 and 15 min, respectively (25 °C). Nickel-mediated reactions were treated with 0.1 M $BuNH_2$ for 30 min at 90 °C.[13] Cleavage products were analyzed on an 8%, 1:20 cross-linked, 50% urea polyacrylamide gel, 0.4 mm thick. Odd-numbered and even-numbered lanes are DNA labeled at the 5′ and 3′ ends with ^{32}P, respectively. Lanes 1 and 2 are DNA control lanes. Lanes 3 and 4 are A specific sequencing reactions.[22] Lanes 5 and 6 contain $CuCl_2$ (2.5 μM) and GGH(Hin139–190) (5 μM) followed by sodium ascorbate (1 mM) and hydrogen peroxide (1 mM). Lanes 7 and 8 are identical with lanes 5 and 6 except that they contain $CuCl_2$ (0.5 μM) and GGH(Hin139–190) (1 μM). Lanes 9 and 10 contain $Ni(OAc)_2$ (5 μM) and GGH(Hin139–190) (5 μM) followed by monoperoxyphthalic acid, magnesium salt (5 μM). Lanes 11 and 12 are identical with lanes 9 and 10 except that they contain $Ni(OAc)_2$ (1 μM), GGH(Hin139–190) (1 μM), and monoperoxyphthalic acid (1 μM). Right: Model of Ni·GGH(Hin139–190) binding to the *hixL* site based on the helix–turn–helix motif in ref 9. The sequence of Hin(139–190) is GRPRAINKHEQEQISRLLEKGHPRQQLAIIFGIGVSTLYRYFPASSIKKRMN. Arrows represent location and extent of cleavage produced by Ni·GGH(Hin139–190) in the presence of monoperoxyphthalic acid.

GGH(Hin139–190) at 1.0 μM concentrations (pH 7.5, 25 °C, 20 mM NaCl) in the presence of $Ni(OAc)_2$ (1.0 μM) and mon-

(1) Mack, D. P.; Iverson, B. L.; Dervan, P. B. *J. Am. Chem. Soc.* **1988**, *110*, 7572.
(2) Camerman, N.; Camerman, A.; Sarkar, B. *Can. J. Chem.* **1976**, *54*, 1309.
(3) Bossu, F. P.; Margerum, D. W. *Inorg. Chem.* **1977**, *16*, 1210.
(4) Bannister, C. E.; Raycheba, J. M. T.; Margerum, D. W. *Inorg. Chem.* **1982**, *21*, 1106.
(5) Sakurai, T.; Nakahara, A. *Inorg. Chim. Acta* **1979**, *34*, L243.
(6) Freeman, H. C.; Taylor, M. R. *Acta Crystallogr.* **1965**, *18*, 939.
(7) Freeman, H. C.; Guss, J. M.; Sinclair, R. L. *Chem. Commun.* **1968**, 485.
(8) Bossu, F. P.; Paniago, E. B.; Margerum, D. W.; Kirksey, S. T.; Kurtz, J. L. *Inorg. Chem.* **1978**, *17*, 1034.

0002-7863/90/1512-4604$02.50/0